Introducing Subgrid-scale Cloud Feedbacks to Radiation for Regional Meteorological and Climate Modeling

Kiran Alapaty[1], Jerold A. Herwehe[1], Tanya L. Otte[1], Christopher G. Nolte[1], O. Russell Bullock[1], Megan S. Mallard[1], John S. Kain[2], and Jimy Dudhia[3]

[1]National Exposure Research Laboratory, U.S. Environmental Protection Agency, Research Triangle Park, North Carolina, USA.

[2]National Severe Storms Laboratory, National Oceanic and Atmospheric Administration, Norman, Oklahoma, USA.

[3]National Center for Atmospheric Research, Boulder, Colorado, USA.

Submitted to *Geophysical Research Letters*
September 26, 2012

Revised on November 6, 2012

Key points: Convective cloud and radiation interaction parameterization improves regional simulations

Abstract

Convective systems and associated cloudiness directly influence regional and local atmospheric radiation budgets, as well as dynamics and thermodynamics, through feedbacks. However, most subgrid-scale convective parameterizations in regional weather and climate models do not consider cumulus cloud feedbacks to radiation, resulting in biases in several meteorological parameters. We have incorporated this key feedback process into a convective parameterization and a radiation scheme in the Weather Research and Forecasting model, and evaluated the impacts of including this process in short-term weather and multiyear climate simulations. Introducing subgrid-scale convective cloud-radiation feedbacks leads to a more realistic simulation of attenuation of downward surface shortwave radiation. Reduced surface shortwave radiation moderates the surface forcing for convection and results in a notable reduction in precipitation biases. Our research reveals a need for more in-depth consideration of the effects of subgrid-scale clouds in regional meteorology/climate and air quality models on radiation, photolysis, cloud mixing, and aerosol indirect effects.

1. Introduction

Clouds and their feedbacks play an important role in the climate system modulating not only the regional and global radiation budgets but also the hydrological cycle [*Stephens*, 2005]. It has been long recognized that radiative feedbacks from clouds affect several meteorological parameters at the surface and aloft through changes in shortwave and longwave radiation locally and globally on short and long timescales [*Shukla and Sud*, 1981]. Also, clouds directly impact air pollutant concentrations by modulating photolysis rates and vertical mixing. Studies on the radiative impacts of cumulus clouds in global climate models emerged in the 1980s [e.g., *Herman et al.*, 1980], while the investigation of the observed nature of the fractional cloudiness

of cumulus convection began at least two decades earlier [*Malkus*, 1958; *Krishnamurti*, 1968]. While explicitly-simulated, resolved-scale clouds were allowed to impact radiation, subgrid-scale cumulus clouds (or parameterized convective clouds) were not. Such radiatively-passive cumulus clouds were prolific at the horizontal resolution used by most global climate models, yet several studies recognized the importance of the radiative impacts of these clouds on the climate system and were unable to model them properly due to lack of a suitable way to estimate fractional cloudiness as a function of parameterized clouds. Based on cloud-resolving modeling studies, *Xu and Krueger* [1991] suggested an empirical formulation to estimate fractional cumulus cloudiness, and it was successfully used in global climate models [e.g., *Collins et al*., 2006; *Neale et al*., 2010]. *Kvamstø* [1993], the first regional modeling study to include cumulus cloudiness, highlighted the advantages of the *Xu and Krueger* [1991] formulation over two other formulations based on grid-scale relative humidity [*Kvamstø*, 1991] and intensity of convection [*Sundqvist et al.*, 1989]. *Pal et al*. [2000] embedded a grid-scale relative humidity based scheme [*Sundqvist et al.*, 1988] directly into a grid-scale cloud and precipitation scheme to implicitly account for subgrid cloud variability impacts in a regional climate modeling study. Based on deep cloud resolving modeling studies, *Xu and Krueger* [1991] showed that the relative humidity is not a suitable parameter to diagnose cumulus cloudiness. *Liang et al.* [2004] proposed an empirical formulation to estimate subgrid-scale cloudiness using a sliding scale approach that accounts for grid resolutions ranging from 200 to 10 km, number of convective layers, and changing some empirical constants. Also, they estimated subgrid-scale condensates independent of the convection scheme used in their study. Despite important findings from these studies, several regional weather models, including Weather Research and Forecasting (WRF), have neglected subgrid-scale cumulus cloudiness and associated radiative impacts. Perhaps it may be

because the overall radiative impacts of subgrid cumulus clouds were thought to be insignificant, at least from a mesoscale weather prediction perspective. Thus, the study focuses on the utility of a robust scheme for estimation of convective cloudiness linked directly to convective cloud dynamical parameters such as suggested *by Xu and Krueger* and an evaluation of impacts of subgrid-scale cloudiness at regional weather and climate scales.

The WRF model [*Skamarock et al*., 2008] is commonly used for retrospective air quality modeling studies [e.g., *Appel et al., 2010*] and is being applied with increasing frequency for historic and future climate studies [e.g., *Otte et al*., 2012; *Nolte et al.,* 2012]. Our regional climate research indicates that the summertime convective systems simulated by the WRF model are highly energetic and often lead to excessive precipitation. We hypothesize that the radiatively passive cumulus clouds result in excessive surface radiant energy. This could manifest as relatively high moist static energy and correspondingly high convective instability and/or unrealistically rapid boundary-layer recovery following parameterized convective events, resulting in more frequent activation of parameterized convection. Given this premise, we further hypothesize that including the effects of subgrid-scale cloudiness in the radiation calculations will alleviate the large precipitation biases in the WRF model by properly reducing shortwave radiation reaching the surface and leading to more appropriate levels of instability and time between parameterized convective episodes in both regional weather and climate simulations.

2. Methodology and Numerical Simulations

In the original WRF (version 3.3.1) model, the grid-scale cloudiness is estimated in a two-stage process. First, if a grid cell is saturated (with respect to water or ice) then that grid cell is assigned 100% cloudiness. Otherwise, that grid cell is assigned 0% cloudiness. Then, the impacts

of other physical and dynamical processes (such as cumulus detrainment, 3-D advection, etc.) on the grid-scale saturation alter the saturation value. This modified saturation value for each grid cell is then utilized to re-estimate partial grid-scale cloudiness using an empirical formulation. Thus, modified grid-scale cloudiness can vary anywhere between 0 to 100% instead of being simply set to binary values. Our analysis has indicated that the modified grid-scale cloudiness still hovers close to either 0% or 100%. This modified grid-scale cloudiness is then taken as input for our research in the estimation of total cloudiness due to all clouds. The subgrid-scale cumulus cloudiness formulation used in the Community Atmosphere Model version 5 (CAM5) [*Neale et al.,* 2010], originally suggested by *Xu and Krueger* [1991], is selected for implementation into the Kain-Fritsch (KF) convection parameterization scheme [*Kain,* 2004] in the WRF model. Following the CAM5 methodology, KF cloud updraft mass fluxes are used to estimate the fractional three-dimensional cloudiness associated with shallow and deep cumulus clouds. Since convection is penetrative, it is allowed to punch through the existing grid-scale clouds. Also, subsidence associated with convection will affect the grid-scale saturation leading to reduction/dissipation of existing grid-scale clouds. The CAM5 formulation accounts for these two types of convection impacts on the grid-scale cloudiness. Finally, grid-scale cloudiness is further modified to ensure that the total cloudiness composed of contributions from grid-scale and subgrid-scale clouds cannot exceed 100%. To maintain consistency, we also adjust grid-scale condensates according to changes made to the grid-scale cloudiness. The standard WRF considers cloudiness only from the grid-scale clouds and associated liquid and ice water paths in radiative transfer calculations. However, to include the radiative contributions by the convective clouds, liquid and ice water condensates associated with the KF subgrid clouds are added to corresponding adjusted grid-scale condensates. Finally, total liquid and ice water paths and

cloudiness values for all clouds are then used in the Rapid Radiative Transfer Model for global (RRTMG) models [*Iacono et al., 2008*] to affect the shortwave and longwave radiative processes. Thus, the modified RRTMG used in the study considers radiative effects of grid-scale as well as subgrid-scale clouds consistent with respective cloud physical formulations.

To understand the effects of radiatively active subgrid clouds, we conducted both weather and regional climate simulations for the continental U.S. using the standard (unmodified) WRF model ("STD") and a version with the subgrid-scale cloudiness feedbacks to radiation ("NEW"). The WRF model configuration included 34 vertical layers extending up to 50 hPa, the Yonsei University planetary boundary layer (PBL) scheme, the Noah land-surface model, and the WSM6 grid-scale microphysics. Two one-week simulations were initialized at 0000 UTC 24 July 2010 to examine model behavior in NWP mode. For these short-term simulations, a single domain with 36-km horizontal grid spacing was used, no data were assimilated (i.e., no interior nudging), and the initial and lateral boundary conditions were derived from the National Centers for Environmental Prediction (NCEP) North American Mesoscale model analyses. Two additional simulations were conducted for a three-year period (1988–1990) to study the subgrid-scale cloudiness effects on regional climate. For the three-year simulations, two-way nested simulations were performed using 108- and 36-km grids. Analysis nudging was applied to horizontal wind components, potential temperature, and water vapor mixing ratio above the PBL toward fields from 2.5° × 2.5° NCEP-Department of Energy Atmospheric Model Intercomparison Project (AMIP-II) Reanalysis (R-2) [*Kanamitsu et al*., 2002] to reduce errors in predictions of means and extremes [*Otte et al*., 2012] and to minimize drift in the large-scale circulation [*Bowden et al*., 2012] for multiyear regional climate simulations.

3. Results

Estimated subgrid cloudiness for the NWP simulations is compared to Geostationary Operational Environmental Satellite (GOES) imagery and against observations from the Surface Radiation (SURFRAD) network. Figure 1a shows the infrared satellite image from GOES-13 valid at 2045 UTC 29 July 2010 and vertically-integrated and normalized (by number of vertical layers) cloudiness for the STD and NEW cases valid at 2100 UTC 29 July 2010. The time shown is about 5 days into the 7-day simulations when the convective activity is predominant as compared to all other days. GOES-13 indicates widespread cloud cover throughout the Sierra Madre Occidental in Mexico and the Rocky Mountain region, in the Upper Midwest, Missouri, southeastward into the Mid-South, along the southwestern Gulf coast of Florida, in the Mid-Atlantic, and off the Atlantic coast. In the STD output cloud coverage is limited to portions of the Upper Midwest, southern Florida, and in the Sierra Madre Occidental (Fig. 1b) where the model produces grid-scale saturation. However, in the NEW output (Fig. 1c) cloud coverage is not limited to those grid points with grid-scale saturation, thus coverage is considerably larger and in much better agreement with observations, particularly through the Rocky Mountains, Missouri, western Tennessee, and offshore in the southern Atlantic Ocean (Figs. 1a, b, c). This comparison indicates that the NEW configuration greatly improves the representation of cloud cover compared to the STD configuration. Improvements in cloud cover with the NEW representation of subgrid-scale clouds occur throughout the simulation period, even for nighttime convective conditions (not shown).

The improved representation of clouds leads to a more realistic depiction of temporal variations in radiative impacts in the NEW. For example, measured surface net shortwave flux at Bondville, Illinois, for 29 July 2010 (Fig. 2a) indicates transient convective cloudiness

throughout the day, resulting in oscillations of more than 200 W m^{-2}. The STD shows an unrealistic smoother distribution with no periods of short-term attenuation during the day because the effect of subgrid cloudiness on radiation is absent. Though the modulation of shortwave radiation in the NEW case is slightly different from observations, it indicates an overall improvement in the temporal variability of shortwave flux. Modulation of surface net longwave flux (Fig. 2b), occurring at an order of magnitude lower than that for shortwave flux, reveals temporal features similar to those of Fig. 2a with a subtle (10-20 W m^{-2}) over-prediction of longwave cooling at this site during the nighttime of 29 July 2010 compared to the STD case and the SURFRAD observations. Further evaluation of short- and long-wave radiative fluxes for all seven SURFRAD sites revealed that these fluxes are better simulated in the NEW case for all-sky conditions while for clear sky conditions fluxes in both the STD and NEW cases are quite similar. Additionally, we have compared the monthly-averaged surface shortwave radiation in STD and NEW at the Bondville site for all three years with the SURFRAD measurements for 15-year monthly climatology. This statistically significant comparison indicated that the surface shortwave radiation in the NEW improves upon STD as NEW is closer to the SURFRAD climatology.

Here we discuss some further prominent results from the STD and NEW cases though space considerations do not permit supporting figures. Since summertime convection is predominant over the eastern U.S., area-averaged differences of surface insolation between the NEW and STD cases were analyzed, revealing local differences of about –80 W m^{-2} that impact simulated surface and PBL parameters. To illustrate the impact of the size of the temperature differences (NEW–STD) on biogenic emissions from an air quality modeling perspective, we chose a small area (400X400 km) over the central North Carolina. For this small area, surface

temperature differences (NEW−STD) indicated a cooling of about 3 K over land, thus indicating the importance of including cloudiness variability and its impact on surface temperatures and related meteorological and air quality parameters. Air pollution can be affected through changes in biogenic emissions, for example, which are controlled by near-surface temperatures. Also, for this seven-day period, eastern U.S. area-averaged PBL depth differences (NEW−STD) range from −100 m to −1200 m indicating cloudiness-radiation impacts on meteorology which would be expected to affect air pollutant concentrations. The NEW case also resulted in a warming (by about 1-3 K with a maximum of about 5 K) of high altitude atmospheric layers (e.g., for the layer 33, which is ~15 km AGL) compared to STD. Temporal variation of domain-averaged (all land grids) layer 33 air temperature differences (NEW−STD) indicates a warming of atmosphere by about 0.2 to 0.4 K starting from the third day of model simulations with a weaker warming during the first two days.. The persistent warming in NEW may be attributed to the introduction of longwave radiative cooling of the deep cumulus clouds acting to warm surrounding regions, which was absent in the STD. Further, warming in NEW can also be attributed to changes in advection patterns because the large-scale dynamics have been altered due to feedbacks associated with the longwave cooling of towering cumulus clouds. Our ongoing research indicates that historical regional climate simulations with WRF for similar periods are biased with excessive areas of cirrus clouds compared with satellite measurements. In the NEW case, upper-level atmospheric warming variably reduced the overprediction of cirrus clouds. After diluting to the resolved scale, domain-maximum subgrid cloud condensate (liquid and solid) in the NEW case is about 1.2 g kg^{-1} (absent in the STD case), an amount that can noticeably alter radiation calculations and saturation levels in the atmosphere. Finally, on average, the NEW case reduced surface precipitation (by about 1 to 20 mm day^{-1} depending up on region and day)

and compares favorably with National Weather Service surface precipitation measurements (Advanced Hydrologic Prediction Service product). Also, the orientation and location of cloud bands (associated with large-scale forcing) corresponded better with satellite imagery than STD (Fig. 1). We now present results obtained from the three-year regional climate simulations.

The 3-year regional climate simulations are evaluated over the southeastern U.S. (where summertime convection is predominant) on a 36-km grid. Prior studies [e.g., *Otte et al*., 2012] indicate that the Southeast is a region with consistent overprediction of summertime precipitation in similar multi-decadal simulations with WRF. Figure 3 compares monthly-averaged surface precipitation for the Southeast from the STD and NEW runs to the North American Regional Reanalysis (NARR; *Mesinger et al*. [2006]). Incorporating subgrid cumulus cloud and radiation interactions mitigates the overprediction of precipitation in all three summers and results in monthly predictions that more closely follow the NARR. The overprediction in the STD case is attributed to radiatively passive subgrid clouds leading to high moist static energy via excessive surface shortwave radiation, which caused strong convective instabilities and increased soil moisture through excessive precipitation. These effects have a positive feedback on the moist static energy and convective kinetic energy leading to overly-intense subgrid convection. The net result is that subgrid convection is highly energetic, leading to an overestimation of surface precipitation in the STD case. This feature becomes evident in the monthly-averaged number of days with surface precipitation exceeding 0.5 inches (12.7 mm) (Fig. 4). Since heavy precipitation is typically associated with intense deep convection, including cumulus cloudiness-radiation interactions has the largest impact on the less frequent heavy precipitation events. Furthermore, the extreme heat events, as measured by the number of days exceeding 90°F, are

higher in NEW than that in STD yet are closer to observations because of smaller surface latent heat fluxes and less soil moisture in NEW.

4. Conclusions

The impacts of including the effects of subgrid-scale cloudiness on radiation fields were examined for weather and climate simulations. For the summertime, we find that including subgrid-scale cloud-radiation interactions improves the simulation of several meteorological parameters at both the weather and climate timescales. Overall, including these effects creates more realistic longwave and shortwave radiation variability, results in cloud patterns which more closely resemble observations, and reduces the overprediction of precipitation (in both monthly averages and for extreme events). This research will directly benefit the regional climate and air quality modeling communities. Radiative feedbacks from subgrid cumulus clouds affect several meteorological parameters important to air quality modeling; such as biogenic emission rates via changes in surface temperature; pollutant concentrations via changes in PBL depth; and peroxide-related reactions through changes in surface humidity levels. Additionally, subgrid cumulus clouds directly impact air pollutant concentrations by modulating photochemistry and vertical mixing. Including the subgrid-scale cloudiness-radiation interactions will also assist the modeling of aerosol indirect effects on parameterized cumulus clouds. In a future study, the impacts of modeling subgrid-scale cloud-radiative feedbacks will be evaluated for air quality simulations with the goal of enhancing the credibility of air quality simulations for retrospective and future periods.

Acknowledgments. The GOES-13 satellite image in Fig. 1 was obtained from the archive maintained by NOAA National Environmental Satellite, Data, and Information Service. The SURFRAD data were made available through NOAA's Earth System Research Laboratory

Global Monitoring Division. Technical feedback on this manuscript was provided by Robin Dennis, Prakash Bhave, and Rohit Mathur (U.S. EPA). The U.S. Environmental Protection Agency through its Office of Research and Development funded and managed the research described here. It has been subjected to the Agency's administrative review and approved for publication.

References

Appel, K. W., S. J. Roselle, R. C. Gilliam, and J. E. Pleim (2010), Sensitivity of the Community Multiscale Air Quality (CMAQ) model v4.7 results for the eastern United States to MM5 and WRF meteorological drivers, *Geosci. Model Dev.*, *3*, 169–188.

Bowden, J. H., C. G. Nolte, and T. L. Otte (2012), Simulating the impact of the large-scale circulation on the 2-m temperature and precipitation climatology, *Clim. Dyn.*, doi:10.1007/s00382-012-1440-y, in press.

Collins W. D., et al. (2006), The formulation and atmospheric simulation of the Community Atmosphere Model version 3 (CAM3), *J. Clim.*, *19*, 2144–2161.

Herman, G. F., M.-L. C. Wu, and W. T. Johnson (1980), The effect of clouds on the earth's solar and infrared radiation budgets, *J. Atmos. Sci*., *37*, 1251–1261.

Iacono, M. J., J. S. Delamere, E. J. Mlawer, M. W. Shephard, S. A. Clough, and W. D. Collins (2008), Radiative forcing by long-lived greenhouse gases: Calculations with the AER radiative transfer models, J. Geophys. Res., 113, D13103, doi:10.1029/2008JD009944.

Kain, J. S. (2004), The Kain-Fritsch Convective Parameterization: An Update, *J. Appl. Meteorol*., *43*, 170–181.

Kanamitsu, M., W. Ebisuzaki, J. Woollen, S.-K. Yang, J. J. Hnilo, M. Fiorino, and G. L. Potter (2002), NCEP-DOE AMIP II Reanalysis (R-2), *Bull. Am. Meteorol. Soc*., *83*, 1631–1643.

309 Krishnamurti, T. N. (1968), A calculation of percentage area covered by convective clouds from
310 moisture convergence, *J. Appl. Meteorol*., *7*, 184–195.
311 Kvamstø, N. G. (1993), An investigation of the cumulus cloudiness parameterization in northerly
312 flows in the Norwegian sea, *Mon. Weather Rev*., *121*, 1434–1449.
313 Kvamstø, N. G. (1991), An investigation of diagnostic relations between stratiform fractional
314 cloud cover and other meteorological parameters in numerical weather prediction models, *J.*
315 *Appl. Meteorol*., *2*, 200–216.
316 Liang, X-Z., L. Li, K.E. Kunkel, M. Ting, and J.X.L. Wang (2004), Regional climate model
317 simulation of U.S. precipitation during 1982-2002. Part I: Annual Cycle. *J. Climate*, *17*, 3510-
318 3529.
319 Malkus, J. S. (1958), On the structure of the trade wind moist layer. *Pap. Phys. Oceanogr.*
320 *Meteorol*., *13*, 1–47.
321 Mesinger, F., et al. (2006), North American Regional Reanalysis, *Bull. Am. Meteorol. Soc*., *87*,
322 343–360.
323 Neale, R. B., et al. (2010), Description of the NCAR Community Atmospheric Model
324 (CAM5.0), NCAR Tech. Note NCAR/TN-486+STR, 268 pp.
325 Nolte, C. G., T. L. Otte, R. W. Pinder, J. H. Bowden, J. A. Herwehe, G. Faluvegi, and D. T.
326 Shindell (2012), Influences of regional climate change on air quality across the continental
327 U.S. projected from downscaling IPCC AR5 simulations, Submitted for inclusion in Air
328 Pollution Modeling and its Application XXII, Springer.
329 Otte, T. L., C. G. Nolte, M. J. Otte, and J. H. Bowden (2012), Does nudging squelch the
330 extremes in regional climate modeling? *J. Clim*., *25*, 7046-7066.

Pal, J.S., E.E. Small, and E.A.B. Eltahir (2004), Simulation of regional-scale water energy budgets: Representation of subgrid cloud and precipitation processes within RegCM. *J. Geophy Res., 105*, 29,579-29,594.

Shukla, J., and Y. Sud (1981), Effects of Cloud-Radiation Feedback on the climate of a general circulation model, J. Atmos. Sci., 38, 2337-2353.

Skamarock, W. C., et al. (2008), A description of the Advanced Research WRF version 3, NCAR Tech. Note NCAR/TN-475+STR, 113 pp.

Stephens, G.L. (2005), Cloud Feedbacks in the Climate System: A Critical Review. J. Climate, 18, 237–273.

Sundqvist, H. (1998), Parameterization of condensation and associated clouds in models for weather prediction and general simulation. Physically-Based Modelling and Simulations of Climate and Climatic Change—Part I. M.E. Schlesinger, Ed., Reidel, 433-461.

Sundqvist, H., E. Berge, and J. E. Kristjansson (1989), Condensation and cloud parameterization studies with a mesoscale numerical weather prediction model, *Mon. Weather Rev*., *117*, 1641–1657.

Xu, K. M., and S. K. Krueger (1991), Evaluation of cloudiness parameterizations using a cumulus ensemble model, *Mon. Weather Rev*., *119*, 342–367.

Figure Captions:

Figure 1: (a) Infrared satellite image from GOES-13 valid at 2045 UTC 29 July 2010; (b) and (c) Vertically integrated and normalized (by number of vertical layers) cloudiness for the STD and NEW cases valid at 2100 UTC 29 July 2010.

Figure 2: (a) Diurnal variation of surface net shortwave radiation (W m^{-2}) at Bondville, IL, from SURFRAD measurements and corresponding simulations in STD, and NEW cases for July 29.

Figure 2: (b) Diurnal variation of surface net longwave radiation (W m^{-2}) at Bondville, IL, from SURFRAD measurements and corresponding simulations in the STD, and NEW cases for July 29.

Figure 3: Temporal variation of monthly area averaged surface precipitation for the southeastern region obtained from the NARR and corresponding simulations in the STD, and NEW cases for three years starting from January 1988.

Figure 4: Temporal variation of monthly area averaged days with surface precipitation exceeding 0.5 inches for the southeastern region obtained from the NARR and corresponding simulations in the STD, and NEW cases for three years starting from January 1988.

Figure 1

(a)

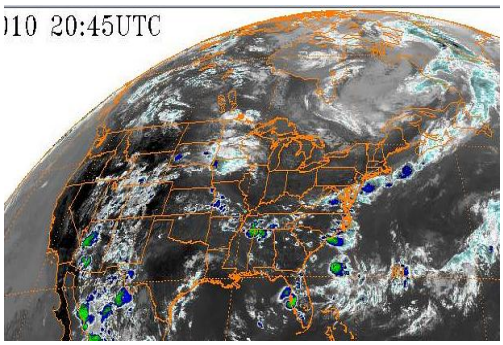

(b)

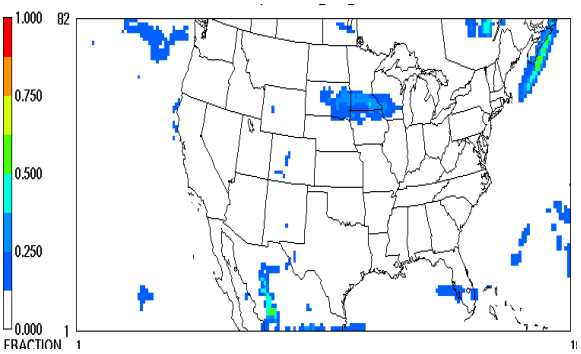

(c)

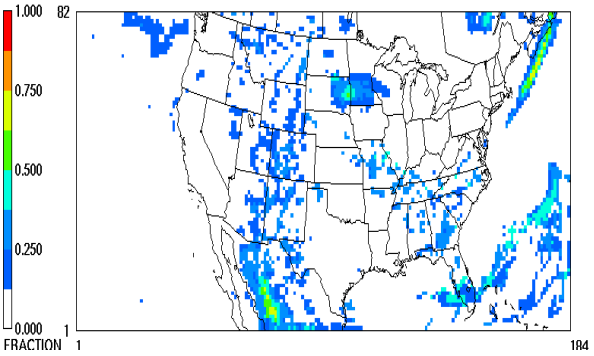

Figure 2

(a)

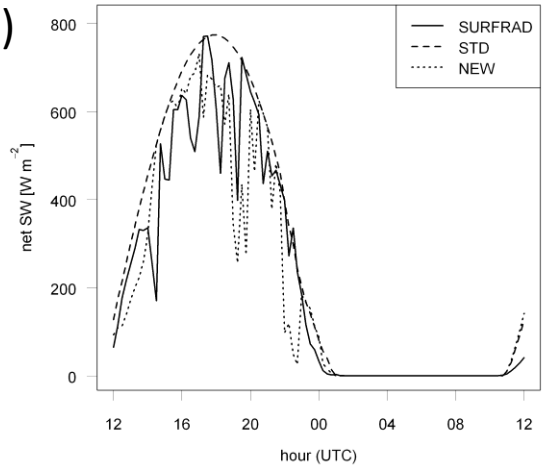

(b)

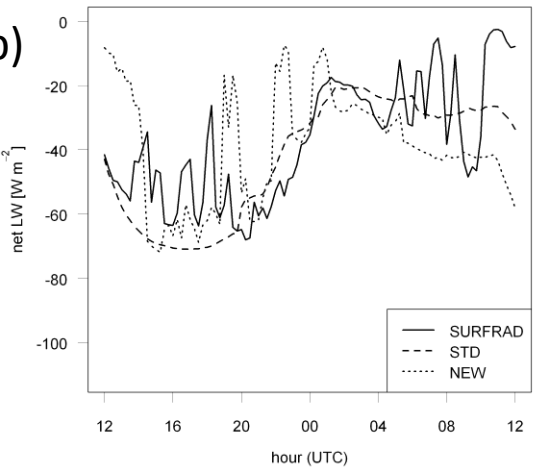

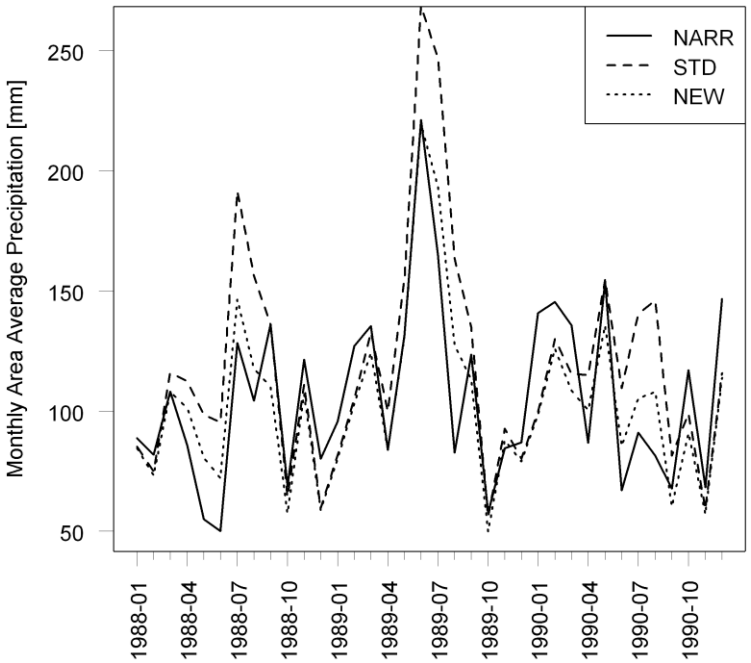

Figure 3

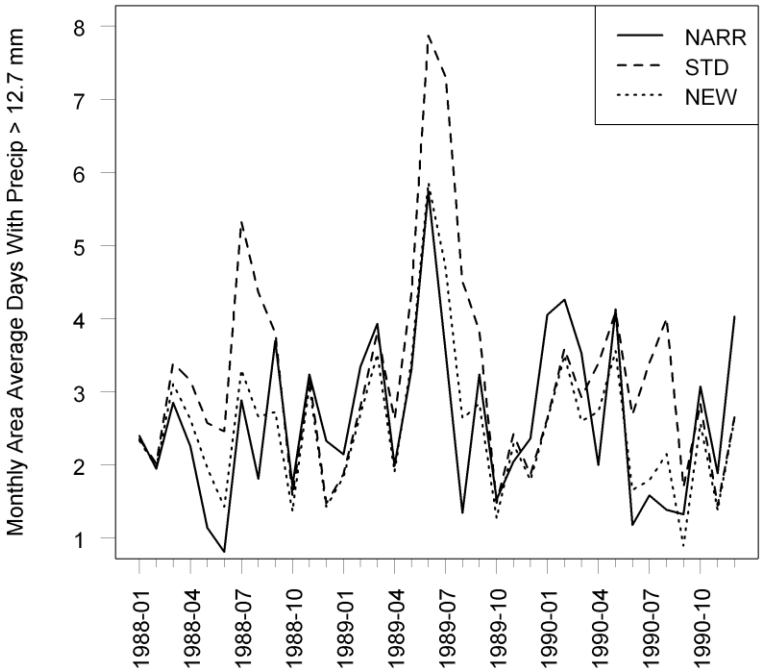

Figure 4